Low Intricacy Multistage Algorithm for Underwater Image Enhancement

by Protek Unkhair

Submission date: 28-Oct-2023 07:00AM (UTC+0700)
Submission ID: 2209534875
File name: 6888-18550-1-SM.docx (11.8M)
Word count: 6524
Character count: 35506

PROtek: Jurnal Ilmiah Teknik Elektro
https://ejournal.unkhair.ac.id/index.php/protk/index

Volume x. No x, May xxxx
e-ISSN: 2527-9572 / ISSN: 2354-8924

Low Intricacy Multistage Algorithm for Underwater Image Enhancement

Ahmed A. Ahmed
Department of Computer Science,
College of Computer Science and Mathematics,
University of Mosul, Iraq
email: ahmed.csp73@student.uomosul.edu.iq

***Zohair Al-Ameen**
Department of Computer Science,
College of Computer Science and Mathematics,
University of Mosul, Iraq
email: *qizohair@uomosul.edu.iq

Abstract **– Humanity currently lives in a technological era that witnesses rapid progress in multiple fields. Digital image processing is one of the modern technologies that has provided practical answers to many challenges including image enhancement, analysis, reconstruction, recovery, compression, processing, and understanding. One of these notable challenges relates to underwater photography. Underwater images are always exposed to less-than-ideal conditions due to environmental and physical factors. These include refraction of light in water, scattering of particles and dust in the aquatic medium, lack of illumination in deep water, and poor contrast. These challenges make it extremely difficult to analyze and extract valuable information without advanced processing. In this study, an improved color balance-fusion algorithm is provided by improving the image visuality and modifying some equations to obtain sharper and clearer images. The proposed algorithm begins by finding the white balance of the input RGB color image, after that, it improves the intensity. Next, the edges are improved using Gamma separately. The weights are then found for each image and combined to find naive fusion. The resulting image is processed using a color retrieval algorithm to produce the final image. along with comparisons to eleven other algorithms with various processing methods. Experimental results showed that this algorithm can significantly improve underwater images, increasing image clarity and making colors clearer. The improvement rates reached 5.8389 and 2.6778 for UISM and UICM metrics, respectively.**

Keywords: underwater, concepts, image enhancement image processing, color images.

I. INTRODUCTION

Digital image processing (DIP) methods have produced practical solutions to a variety of problems, including picture enhancement, analysis, reconstruction, restoration, manipulation, and many more. These difficulties can be found in a variety of image-related applications, underwater imaging being one of them. Experts' attention has recently been drawn to the processing of underwater photographs due to the widespread use of DIP in this area [1-3]. The quality of underwater photographs is vital in scientific pursuits like watching marine life, counting populations, and studying geological or biological conditions. The main challenge in obtaining underwater photographs is the haziness caused by light that reflects off the ocean's surface and is subsequently bent and scattered by water molecules. Additionally, because different wavelengths of light absorb light differently, there are color variances [4-6]. Due to light scattering and color alterations, images captured underwater suffer from contrast loss and color divergence. Sand, minerals, and plankton, which are present in lakes, oceans, and rivers, are among the suspended particles that contribute to murkiness.

These suspended particles cause a small portion of the light that is reflected from objects and moving toward the camera to collide. As seen in Figure 1, different wavelengths of light are attenuated in the water body in different ratios. Due to this uneven attenuation, color bias is frequently visible in underwater photographs. The degeneration of underwater images can also be caused by suspended particles in the water. Figure 1 illustrates how nearby particles affect incident light's small-angle scattering (forward scattering) while nearby particles affect ambient light's large-angle scattering (backscattering), which enters the camera lens. These light refractions result in grainy and blurry underwater photographs. Figure 1 depicts the installation of artificial lighting systems to provide the necessary illumination for the gloomy deep-sea environment as underwater missions go deeper. In Figure 2, various underwater image samples are provided.

Low visibility is a result of backscattering and light attenuation, which is problematic for underwater photography. Random light attenuation causes the illusion of murkiness. Some of the light reflecting from the medium along the line of sight reduces the contrast of recorded images. Different undersea ecosystems have various basic visual degeneration causes. Recently, several strategies to enhance the caliber of underwater photos have been suggested by researchers [8-10].

http://doi.org/10.33387/protk.vxix.xxxx

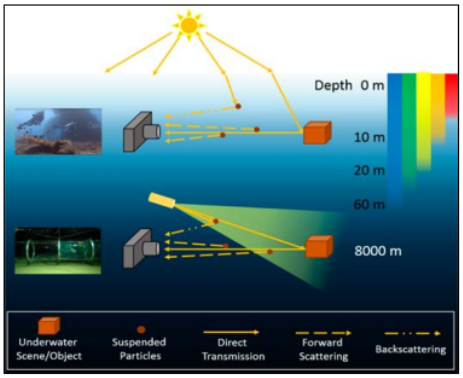

Figure 1. Underwater optical imaging in shallow water and deep sea [7].

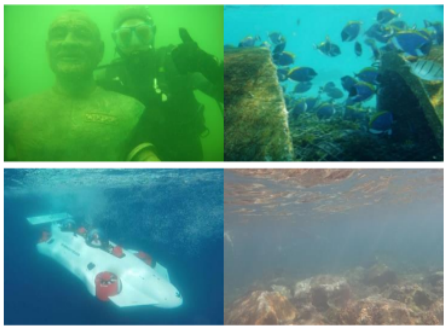

Figure 2. Samples of different underwater images.

II. Literature Review

Various research works related to enhancing underwater images are reviewed to deliver the necessary knowledge of the previously developed underwater enhancement algorithms. The major goal of this study is to identify previously employed concepts and assess their benefits and drawbacks to facilitate a thorough understanding of processing notions, making the improvement procedure simpler. Additionally, both the benefits and drawbacks are considered, with the benefits being completely utilized and the drawbacks being carefully avoided. In 2012 [11], it initially used the existing dark channel scene depth derivation method to estimate and calculate the separation between the subject and the camera to get the derived depth map (DDM). Using the DDM, the front, and back regions within the image are divided into two parts. The influence of haze and color change from the object to the camera is subsequently eliminated using a drying algorithm for wavelength adjustment. The depth of the water is then determined by dividing the remaining power across the several color channels in the back. To modify the blue tone to its true color, each color is then compensated for each channel.

In 2013 [12], proposed a UDCP algorithm that utilizes the standard DCP in an exceptional way for underwater images, in that the DCP concept is only implemented on the image's green and blue channels as these two layers are vastly affected by the high absorption effect related to underwater conditions. In the UDCP, dark areas are detected using a specialized approach with is different from the one used by the standard DCP. In addition, it utilizes a spectral matting approach to enhance the approximation of transmission which is considered an important phase in the standard DCP.

In addition, in 2017 [13] the BLA was introduced, in that it generates an enhanced image using three steps. The first step involves computing the noise map and then processing it with a Gaussian filter. Next, the max filter is used to approximate the blur map followed by determining the blurriness (B) using the guided filter. The second step involves determining the light absorption amount by selecting background light from the hazy image regions to be used next in obtaining the transmission map (TM). The third step involves creating the out image using TM, B, and the original image. In 2017 [14] proposed TSA, which utilizes two basic principles of color correction and contrast enhancement. For the first step, it utilizes piecewise linear approach on the saturation channel of the input image for color correction. Next, the image is transformed to the LAB domain, and an adaptive histogram equalization is applied to improve contrast. Finally, the final image is acquired by converting the filtered image to RGB.

Furthermore, in 2018 [15], a DHW algorithm was introduced, in that it first uses an end-to-end convolutional neural network to estimate the "transmission map" (TM). It also makes use of the bilateral adaptive filter to improve the TM. Moreover, a color aberration removal strategy based on white balance is utilized for color enhancement. Next, the Laplace hierarchy is applied to obtain a sharper image. Finally, the hybrid wavelets concept is used to generate the output image. Moreover, in 2019 [16], the GIF method was developed, in that white balancing is initially performed on the input image for initial image adjustment. Then, the adjusted image is obtained, and two images are generated from it, one having better sharpness and the other one owning a corrected gamma. Next, for both images, the weight map is generated after detecting the salient features using a directed filter. The final image is generated using the weight generated weight maps when merging the sharpened and the gamma-corrected images.

In 2020[17], introduced HF, in that the input image is initially processed by underwater white balance (UWB). UWB consists of four main steps: color compensation, histogram stretching, gray-world approach, and mapping. The output of UWB is then processed by a guided filter and sent to the variational contrast and saturation enhancement (VCSE) phase along with the input image. VCSE is an approach that improves the contrast and saturation of the image through multiple iterations to generate the final image. Moreover, in 2021[18], a hybrid approach was proposed, in that the dark channel prior method is applied to the blue channel instead of the red channel due to the unstable density of the red channel in the aquatic environment. It involves splitting the image

into patches, calculating the light amount for each patch, and smoothing the transmission map via a directed filter. The image is then converted to the HSV color model, and a linear stretching approach is applied to all the channels. Next, contrast stretching is applied to the saturation and value channels and the image is converted back to the RGB domain to generate the output image.

Lastly, in 2022 [19], the MWMGF approach is introduced, it first corrects the colors by using color weight balance and adaptive histogram equalization. From the previous step, different weights are determined which are Laplace contrast, local contrast, saliency, saturation, and exposure weights. Having the input and processed images with the computed weights, the output image is generated using a multigrain fusion procedure. Different approaches from the methods under investigation have been used previously to filter underwater images and provide satisfactory results. The reviewed studies are listed in Table 1 in chronological order, along with the authors, years, concept, intricacy, pros, and cons.

Table 1. The reviewed methods synopsis.

Method	Concept	Intricacy	Pros	Cons
WCD [11]	Wavelength compensation and dehazing	Moderate	Preserve the color of the image	relatively large white shiny regions
UDCP [12]	dark channel prior	Low	high speed	limited in underwater conditions
BLA [13]	Blurriness and light absorption	Moderate	Increase the Contrast	much complicated
TSA [14]	Color and contrast correction	Low	high speed	unnatural contrast
DHW [15]	DehazeNet and hybrid wavelets	High	the best performance in terms of the GLCM features and DMOS.	increasing color distortion
GIF [16]	white balancing, sharpening, and gamma correction	High	work well on images that have more of a blue color composition	increase in white-balance
HF [17]	white balance with variational contrast and saturation enhancement	Moderate	improvements in contrast and saturation	cannot image recognition and target detection
HA [18]	dark channel prior with guided filter	Moderate	good output image contrast and high-speed	unclear background objects
MWMGF [19]	multi-weight and multi-granularity fusion	High	Balanced CE	some noise is amplified

III. PROPOSED ALGORITHM

The main aim of the proposed algorithm is to recover adequate quality underwater images from their distorted versions with as many details and color information as possible. As stated in the literature review, different algorithms have been proposed for underwater images, yet not all attained the anticipated results and hence, the opportunity still stands to develop an algorithm for better underwater image enhancement. For this purpose, a thorough search for an algorithm to be developed has been made and an algorithm named color balance and fusion (CBF) [20] has been selected as the CBF has a low-complexity structure, color correction phase, contrast adjustment step, sharpness enhancement phase, and a simple image fusion approach.

This algorithm simply works as follows: it begins by receiving the input image. Then, a white-balancing process is applied to correct the colors and reduce the color cast produced by the light scattering in the underwater environment. Next, two images are derived from the results of the previous step, in that the first image is processed by a gamma correction approach to adjust the color contrast while the second image is sharpened using a normalized unsharp masking filter to increase the acutance of details. Next, the weighting maps the normalized weights for both maps are determined to be fused. Accordingly, a naive fusion approach is implemented to blend the normalized weights with the sharpened and contrast-enhanced images to the output image that has better colors, tuned contrast, and better acutance. Figure 3 shows the diagram of the CBF algorithm.

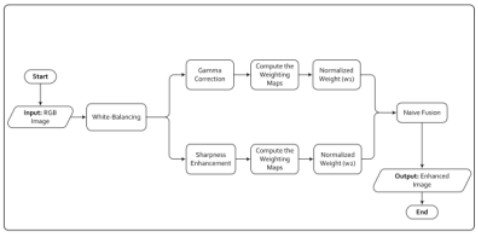

Figure 3. Diagram of the CBF algorithm.

A detailed explanation of the CBF algorithm goes as follows: the algorithm receives a color RGB underwater image (I) in the range [0,1] and starts the white balancing (WB) step, which includes the red color compensation (RCC) step followed by the application of a gray world (GW) algorithm to produce the color-balanced image. Accordingly, the WB step begins by splitting the image into its three main channels Red I_r, Green I_g, and Blue I_b. Next, the mean value for each channel is computed as μ_r for I_r, μ_g for I_g, and μ_b for I_b. The mean is computed by summing all the channel pixel values and then dividing them by the number of pixels in that channel. The RCC step considers the following issues: the green channel is highly maintained in the underwater image, so the green channel will not be modified. Instead, it will be used as is as well, and it will be utilized to majorly compensate the red channel I_{rc} and slightly compensate the blue channel I_{bc}. Such step can be mathematically computed using the following equations:

$$I_{rc} = I_r + \alpha \cdot (\mu_g - \mu_r) \cdot (1 - I_r) \cdot I_g \quad (1)$$

$$I_{bc} = I_b + \alpha \cdot (\mu_g - \mu_b) \cdot (1 - I_b) \cdot I_g \quad (2)$$

where α is a scalar that is α = 0.1. After the above-mentioned compensation step, a color RGB image (W) is formed from red I_{rc}, green I_g, and blue I_{bc}. Next, the GW algorithm [21, 22] is implemented as follows: it receives the image (W) in an RGB form and linearizes and gamma-corrects the RGB values then computes the mean value for each layer (μ_{Wr}, μ_{Wg}, μ_{Wb}) in this image. Next, it computes the average gray value using the following equation:

$$G = \frac{\mu_{Wr} + \mu_{Wg} + \mu_{Wb}}{3} \quad (3)$$

After that, it computes the scalar values (S_{v1}, S_{v2}, S_{v3}) that are used to adjust each channel using the following equations:

$$S_{v1} = \frac{G}{\mu_{Wr}} \quad (4)$$

$$S_{v2} = \frac{G}{\mu_{Wg}} \quad (5)$$

$$S_{v3} = \frac{G}{\mu_{Wb}} \quad (6)$$

After that, each layer is adjusted using the following equations:

$$L_r = S_{v1} \cdot W_r \quad (7)$$

$$L_g = S_{v2} \cdot W_g \quad (8)$$

$$L_b = S_{v3} \cdot W_b \quad (9)$$

where, L is the resulting image from the GW algorithm (W_r, W_g, W_b) are the linearized gamma-corrected red, green, and blue channels of image W. Next, the result (L) of the GW algorithm is further adjusted using a chromatic adaptation (CA) approach with a Bradford model [23]. The CA approach is an event that retains the color look nearly constant through fluctuations in the color of the illuminated [24]. It is necessary to use CA so that the colors appear more correct to the viewer. The CA approach includes the following steps: (1) transform the image to Bradford cone response domain; (2) scale elements by certain factors; (3) apply the inverse transform. After that, the gamma correction approach is applied to the linear RGB values to produce an output image (Q) in the standard RGB format, which is appropriate for display.

After the completion of the white balancing step and obtaining image (Q), two processes of color contrast enhancement and image sharpening are applied independently on the white balanced image (Q) to produce two different images that are fused using a naive image fusion procedure. To improve the color contrast, a gamma correction process is applied as the image (Q) tends to appear somewhat bright and gamma correction can reduce such unwanted brightness while increasing the contrast for better detail representation. The utilized gamma correction approach can be expressed as follows [25]:

$$G = c \cdot Q^{\gamma} \quad (10)$$

where c and γ are two scalars that control the curve shape of the above approach, and G is the gamma-corrected image. As for the sharpening procedure, a normalized unsharp mask (NUM) filter is applied as it does not introduce the unwanted effects of the standard unsharp mask filter, and it is fully automated and does not need parameter tuning as well. The NUM filter can be expressed as follows [26]:

$$A = \frac{(Q + \mathrm{N}\{Q - K\})}{2} \quad (11)$$

where A is the sharpened image, K is a Gaussian filtered counterpart of image Q, and $N\{.\}$ is a linear normalization process. The normalization helps in rescaling the color values to the full range so that the image's visual details are represented in a better way. At this point, the weighing maps and the normalized weights for images G and A must be determined. For that, images A and G are converted from the RGB domain to the LAB domain, and the (L) channel is adopted as E_1 for A and E_2 for G, in that (R_1=E_1/255) and (R_2=E_2/255), as R_1 and R_2 represent the luminance of each image. Next, the Laplacian contrast weight (LCW) is computed to approximate the global contrast using the luminance layers R_1 and R_2 as follows:

$$LCW_1 = |R_1 * K_L| \quad (12)$$

$$LCW_2 = |R_2 * K_L| \quad (13)$$

where, K_L is the Laplacian kernel [1, 1, 1; 1, -8, 1; 1, 1, 1], and (*) is a convolution operation. Next, the saliency weight (SYW) is determined for both images A and G to highlight the salient items that their eminence is attenuated when captured in an underwater environment. This is done using a frequency-tuned (FT) algorithm for salient area recognition proposed by [27]. Both G and A images must be processed by the FT algorithm to produce two saliency weights that are needed later when computing the normalized weights required for the fusion process.

Let's denote the input to the FT algorithm as F, the FT algorithm works as follows: Firstly, image F is first filtered by a Gaussian low pass filter to produce a blurry version of F denoted as FG. Next, image FG is converted to the LAB color space, to get three channels of L_{FG}, A_{FG}, and B_{FG}. After that, the mean value for each channel is determined as (μ_L, μ_A, μ_B) to be used to compute the saliency weight as follows:

$$SYW = (L_{FG} - \mu_L)^2 + (A_{FG} - \mu_A)^2 + (B_{FG} - \mu_B)^2 \quad (14)$$

When the above-mentioned steps are applied to image A, its saliency weight is denoted as SYW_1, and when applied to image G, its saliency weight is denoted as SYW_2. After that, the saturation weight (SAW) must be determined as well for both images A and G, as it allows the fusion process to adjust to chromatic data by utilizing the extremely saturated areas in the image.

$$SAW_1 = \sqrt{\frac{(A_r - R_1)^2 + (A_g - R_1)^2 + (A_b - R_1)^2}{3}} \quad (15)$$

$$SAW_2 = \sqrt{\frac{(G_r - R_2)^2 + (G_g - R_2)^2 + (G_b - R_2)^2}{3}} \quad (16)$$

Next, the normalized weights NW_1 and NW_2 are computed from the above-stated weights to be used in the fusion process as follows:

$$NW_1 = \frac{LCW_1 + SYW_1 + SAW_1 + 0.1}{LCW_1 + SYW_1 + SAW_1 + LCW_2 + SYW_2 + SAW_2 + 0.2} \quad (17)$$

$$NW_2 = \frac{LCW_2 + SYW_2 + SAW_2 + 0.1}{LCW_1 + SYW_1 + SAW_1 + LCW_2 + SYW_2 + SAW_2 + 0.2} \quad (18)$$

Finally, a naive fusion (*NF*) process is applied to reconstruct a better image using the predetermined normalized weights using the following equation [28]:

$$NF = (NW_1 \cdot A) + (NW_2 \cdot G) \quad (19)$$

where *NF* represents the enhanced underwater image. When dealing with underwater images, the CBF algorithm may show some drawbacks as mentioned earlier. Therefore, a newly developed algorithm is introduced to adequately process various underwater images based on the CBF model and other adequate processing concepts to achieve better results. The proposed algorithm is expected to process many underwater images and produce results with good color, normal contrast, few impurities, and good brightness. The developments on the CBF are as follows: Firstly, instead of using gamma correction, an ABCETP algorithm developed by [29], is utilized with a TGA process to improve the contrast and brightness. Secondly, instead of using the NUM filter, an ADUSM filter proposed by [30], is used instead to provide a better sharpness. Finally, a color restoration step proposed by [31], is used as a final step to improve the colors and produce better results. Figure 4 shows the diagram of the proposed algorithm.

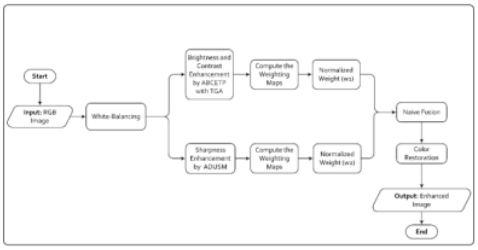

Figure 4. Diagram of the developed algorithm.

As for the ABCETP [29], (A) stands for ameliorated, (BCET) stands for balance contrast enhancement technique, and (P) stands for parabolic function. It begins by receiving the input image (X), contrast enhancement parameter (λ), and brightness enhancement parameter (δ), and setting these parameters as L=0 and H=1. Next, it finds the standard deviation (ς) and the discrete entropy (η) from the input image as follows:

$$\varsigma = \sqrt{\frac{1}{N-1}\sum_{i=1}^{N}|x_i - \mu|^2} \quad (20)$$

$$\mu = \frac{1}{N}\sum_{i=1}^{N} x_i \quad (21)$$

$$\eta = \sum p(x_i)\log_2 p(x_i) \quad (22)$$

where $p(x_i)$ represents the x_i probability density function; xi is the input image in a vector form. After that, the three ABCETP coefficients are computed using the following equations:

$$\dot{B} = \frac{h^2(\lambda) - \eta + l^2(1-\lambda)}{2[h(\lambda) - \varsigma + l(1-\lambda)]} \quad (23)$$

$$A = \frac{H - L}{(h-l)(h+l-2\dot{B})} \quad (24)$$

$$C = 1 - A(l - \dot{B})^2 \quad (25)$$

where h and l are the highest and lowest values X. Following, the modified parabolic function as follows:

$$\dot{Y} = A(\sinh(X) - \dot{B})^2 + C \quad (26)$$

After that, a post-processing phase is implemented which includes the following equations:

$$G = 1 - \frac{\exp(-\delta\dot{Y})}{(1 + \exp(-\dot{Y}))^{\delta}} \quad (27)$$

$$\alpha = \frac{1}{\max(G) - \min(G)} \quad (28)$$

$$\beta = \frac{\min(G)}{\max(G) - \min(G)} \quad (29)$$

$$R = \alpha * G - \beta \quad (30)$$

Next, a transform gamma adjustment (TGA) process is applied to further adjust the output of the ABCETP algorithm. The TGA is computed as follows [32] :

$$TGA = \max(R) * \left(\frac{R}{\max(R)}\right)^{\gamma} \quad (31)$$

where TGA is the output image and γ is a scalar. For most images, the value of γ = 2. As for the ADUSM [30], (AD) stands for anisotropic diffusion, and (USM) is unsharp masking. ADUSM starts by getting the input image $f_{i,j}$ and the sharpness parameter (λ), setting the iterations to 20, computing the image size, and determining the smoothness parameter K. Next, an iterative process starts and the first issue to be calculated is the neighbor differences in four directions using the following equations:

$$\nabla_N I_{i,j} = I_{i-1,j} - I_{i,j} \quad (33)$$

$$\nabla_S I_{i,j} = I_{i+1,j} - I_{i,j} \quad (34)$$

$$\nabla_E I_{i,j} = I_{i,j+1} - I_{i,j} \quad (35)$$

$$\nabla_W I_{i,j} = I_{i,j-1} - I_{i,j} \quad (36)$$

where, $f_{i,j} = I_{i,j}$ at iteration one only. $I_{i,j}$ is a filtered image in every iteration. Next, the conduction operators are computed using the following equations:

$$g_N = \frac{1}{1 + \left(\frac{\nabla_N I_{i,j}}{K}\right)^2} \quad (32)$$

$$g_S = \frac{1}{1 + \left(\frac{\nabla_S I_{i,j}}{K}\right)^2} \quad (37)$$

$$g_E = \frac{1}{1 + \left(\frac{\nabla_E I_{i,j}}{K}\right)^2} \quad (38)$$

$$g_W = \frac{1}{1 + \left(\frac{\nabla_W I_{i,j}}{K}\right)^2} \quad (39)$$

$$K = 2 * \left[\frac{\text{mean}(f_{i,j})}{(0.75 * \varsigma(f_{i,j}))} \right] \quad (40)$$

where ς represents the standard deviation. After that, the smoothed image is determined using the following equation:

$$I_{i,j} = I_{i,j} + 0.25 * \left[\begin{matrix} (g_N * \nabla_N I_{i,j}) + (g_S * \nabla_S I_{i,j}) + \\ (g_E * \nabla_E I_{i,j}) + (g_W * \nabla_W I_{i,j}) \end{matrix} \right] \quad (41)$$

Finally, the USM filter is computed as follows:

$$Q_{i,j} = f_{i,j} + \lambda [f_{i,j} - I_{i,j}] \quad (42)$$

where, $Q_{i,j}$ is the output image of ADUSM. As for the color restoration step, the method proposed by [31] has been utilized, in that it receives the input image NF and divides it by three to get image av. Next, it computes parameters c and v that will be used in color restoration as follows:

$$v = NF_r + NF_g + NF_b \quad (43)$$

$$c = \log(128 * t + 1) + \log(v + 1) \quad (44)$$

where, NF_r, NF_g, and NF_b are the red, green, and blue layers of NF, and t is NF_r. Next, a gamma correction step is implemented as follows:

$$avc = (av * c)^{\gamma} \quad (45)$$

where γ has the same value as the γ in Eq (31). Following, the range for color correction is computed as follows:

$$rn = \left([\mu(avc) + \varsigma(avc) * d] \right) - \left([\mu(avc) - \varsigma(avc) * d] \right) \quad (46)$$

where μ represents the mean, ς is the standard deviation, and d is a scalar that represents the amount of color restoration in that ($d > 0$), and a higher value gives more colors to the recovered image. At this point, if $rn = 0$, then it would become $rn = 1$ to avoid the division by 0 in the following step. The final restored image is obtained using the following equation:

$$res = 255 * \left(\frac{avc^2 - \left([\mu(avc) - \varsigma(avc) * d] \right)}{rn} \right) \quad (47)$$

where res is the output image of the algorithm.

IV. Results and Discussion

In this section, the outcomes and related remarks are presented to analyze and demonstrate the processing capabilities of the developed algorithm with a dataset of degraded underwater images. The dataset comprising 950 authentic underwater images was utilized. These images were split into two segments: the first section contained 890 images, each paired with corresponding reference images. The remaining 60 images posed a challenge as satisfactory reference images were challenging to obtain, and all these images exhibited natural degradation. It's important to note that the dataset consisted of 890 original underwater images, totaling approximately 630MB, and their respective reference images, totaling approximately 786MB [33].

For measurement purposes, UISM and UICM are used as important tools for objectively assessing the performance of different algorithms or techniques. Researchers use these metrics to quantitatively compare the quality of processed images with their original counterparts or reference images, especially the underwater images. Higher UISM scores indicate better preservation of structural details, while higher UICM scores suggest more accurate and pleasing colors in the processed images. These metrics allow researchers to make informed judgments about the strengths and weaknesses of each algorithm and how they impact image quality in both structural and color aspects.

The experimental results showed that the developed algorithm has promising abilities in processing different degraded underwater images as the results own good colors, sharp edges, better brightness, improved contrast, and no obvious processing errors, and they appear more credible to the viewer. Accordingly, when comparing the unprocessed Image with its processed version, it seems as if a layer of distortions has disappeared, and the true color of the image have been restored. The development algorithm depends on the d value that the operator chooses to retrieve the color of the underwater image. Figures (5 to 8) demonstrate the degraded images and their filtered versions by the developed algorithm.

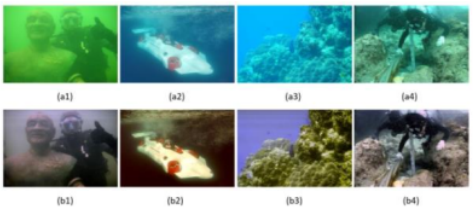

Figure 5. The outcomes of the developed CBF algorithm. (a) degraded underwater images; (b) resulting images by the proposed algorithm with d = 17, 8, 20, and 18, respectively.

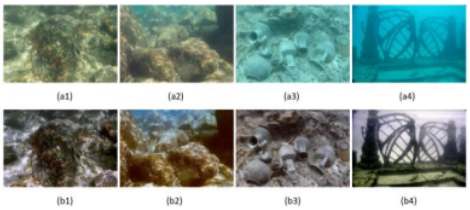

Figure 6. The outcomes of the developed CBF algorithm. (a) degraded underwater images; (b) resulting images by the proposed algorithm with d = 25, 19, 18, and 23, respectively.

By looking at the results in Figures 4 to 7, it was found that a variety of distorted underwater images were used. Emphasis has been placed on images with green and blue colors because these colors retain their details better in a water environment since the red color loses its effect first due to its higher absorption of water. Images were also taken in different conditions including day and night and at varying water depths. The results show that the developed

algorithm significantly improved the quality of the distorted images. The algorithm was able to highlight details in the image remarkably and increase its clarity. The contrast is well-adjusted, colors are improved, and brightness and distortion issues have also been addressed. One notable achievement of the algorithm is effective color retrieval. This was done by determining the appropriate d value for each image, which varied based on the image's contrast, depth, and dominant color.

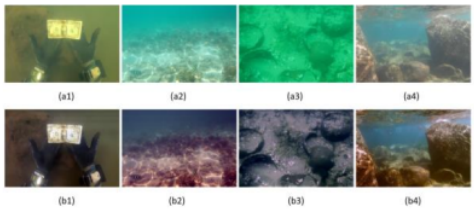

Figure 7. The outcomes of the developed CBF algorithm. (a) degraded underwater images; (b) resulting images by the proposed algorithm with d = 7, 30, 30, and 16, respectively.

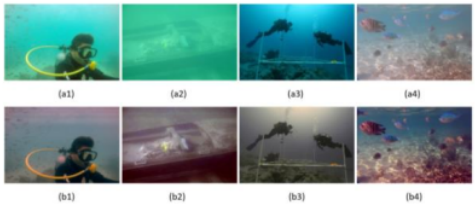

Figure 8. The outcomes of the developed CBF algorithm. (a) degraded underwater images; (b) resulting images by the proposed algorithm with d = 9, 37, 20, and 18, respectively.

By looking at the results in Figures 4 to 7, it was found that a variety of distorted underwater images were used. Emphasis has been placed on images with green and blue colors because these colors retain their details better in a water environment since the red color loses its effect first due to its higher absorption of water. Images were also taken in different conditions including day and night and at varying water depths. The results show that the developed algorithm significantly improved the quality of the distorted images. The algorithm was able to highlight details in the image remarkably and increase its clarity. The contrast is well-adjusted, colors are improved, and brightness and distortion issues have also been addressed. One notable achievement of the algorithm is effective color retrieval. This was done by determining the appropriate d value for each image, which varied based on the image's contrast, depth, and dominant color.

This contributed to improving the representation of colors and showing them accurately. Overall, it can be concluded that the developed algorithm has performed well in improving the quality of underwater images and achieving significant improvements in detail, contrast, and colors. In addition to what was mentioned above, the analysis also indicates that the developed algorithm was able to deal with special challenges faced in photographing underwater objects. For example, the effect of refraction of light in water, which significantly distorts images, has been successfully dealt with. This effect is corrected, and the overall clarity of the images is improved. In addition, advanced techniques have been applied to remove distortions caused by variable factors in the aquatic environment such as floating particles and plankton. The algorithm was able to improve the clarity of images and reduce blur related to these factors. From Figures 9 to 15 and Tables 2 to 4, it is spotted that dissimilar outcomes are obtained, as different algorithms in concept were implemented with numerous underwater images. In this comprehensive evaluation of various image enhancement algorithms, we aimed to assess their performance across different metrics and criteria.

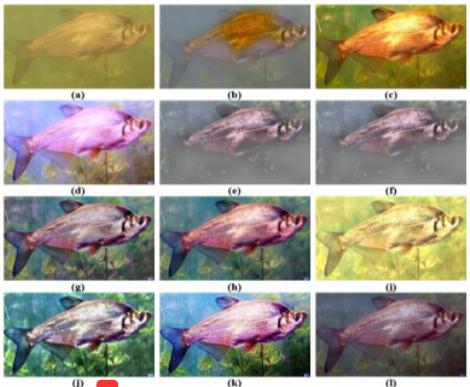

Figure 9. The comparison outcomes (Set 1). (a) real-degraded underwater image; the following images are enhanced by: (b) WCD, (c) UDCP, (d) BLA, (e) TSA, (f) DHW, (g) GIF, (h) HF, (i) HA, (j) MWMGF, (k) CBF (original), (l) Our method.

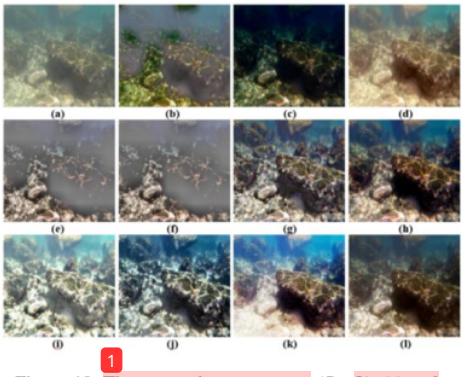

Figure 10. The comparison outcomes (Set 2). (a) real-degraded underwater image; the following images are enhanced by: (b) WCD, (c) UDCP, (d) BLA, (e) TSA, (f) DHW, (g) GIF, (h) HF, (i) HA, (j) MWMGF, (k) CBF (original), (l) Our method.

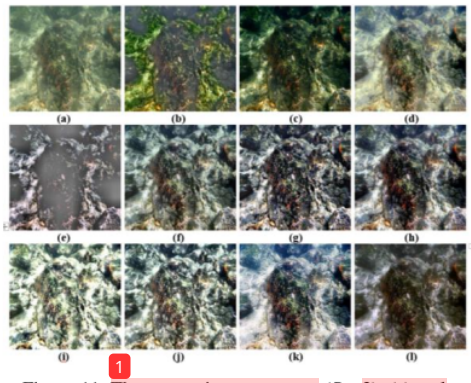

Figure 11. The comparison outcomes (Set 3). (a) real-degraded underwater image; the following images are enhanced by: (b) WCD, (c) UDCP, (d) BLA, (e) TSA, (f) DHW, (g) GIF, (h) HF, (i) HA, (j) MWMGF, (k) CBF (original), (l) Our method.

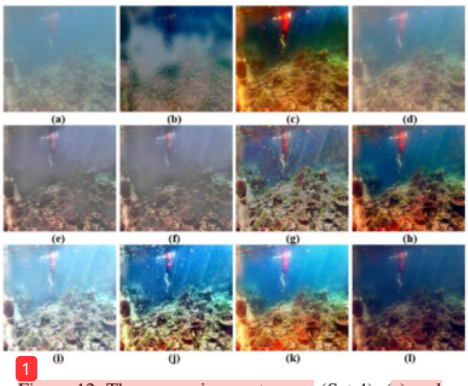

Figure 12. The comparison outcomes (Set 4). (a) real-degraded underwater image; the following images are enhanced by: (b) WCD, (c) UDCP, (d) BLA, (e) TSA, (f) DHW, (g) GIF, (h) HF, (i) HA, (j) MWMGF, (k) CBF (original), (l) Our method.

Table 2. The recorded accuracies of the UISM metric ↓.

No.	Original CBF	MWMGF	HA	HF	GIF	DHW	TSA	BLA	UDCP	WCD	Proposed
Img1	6.5699	6.8787	6.561	6.671	6.5853	6.7271	5.2798	6.7324	6.794	6.7861	6.6299
Img2	8.8322	5.8341	9.717	8.748	5.9236	5.1271	7.2224	9.6987	8.822	9.0664	5.4222
Img3	8.8248	6.2398	8.941	8.677	6.5711	6.4777	7.5595	8.6912	8.792	8.9616	6.4244
Img4	8.8648	5.6674	12.183	8.765	5.7258	5.7439	8.6661	10.462	10.25	8.4744	4.8791
Ava.	8.2729	6.155	9.350	8.215	6.20145	6.01895	7.18195	8.89617	8.6651	8.32212	**5.8389**

Table 3. The recorded accuracies of the UICM metric↑.

No.	Original CBF	MWMGF	HA	HF	GIF	DHW	TSA	BLA	UDCP	WCD	Proposed
Img1	-0.0223	-28.916	12.088	-0.002	-0.6639	-27.114	0.010	0.0907	0.133	0.013	4.6398
Img2	-0.0049	-17.688	-13.23	0.0077	1.4135	-17.502	0.008	0.0497	-0.077	-0.024	2.7747
Img3	-0.0158	-8.2053	-12.15	-0.007	-1.9341	-8.5571	0.003	-0.0305	-0.069	-0.047	0.2891
Img4	-0.0031	-46.070	-34.55	-0.031	0.5582	-46.503	0.010	-0.032	0.096	-0.084	3.0076
Ava.	-0.0115	-25.220	-22.59	-0.008	-0.1565	-24.919	0.008	0.0194	0.020	-0.035	**2.6778**

Table 4. The Application Times (in Seconds) for the Comparison Algorithms ↓.

No.	Original CBF	MWMGF	HA	HF	GIF	DHW	TSA	BLA	UDCP	WCD	Proposed
Img1	0.70503	2.00621	0.6114	7.0605	2.4459	2.8673	1.2968	13.433	3.7137	1.3188	0.777
Img2	1.29190	2.44753	0.6647	17.701	4.4988	3.2457	2.9846	33.015	4.1931	1.5652	1.3597
Img3	1.35398	1.51956	0.6250	15.595	2.7277	4.3321	3.5815	33.974	3.6417	1.3392	1.7178
Img4	1.26778	2.51471	0.7043	17.959	2.7875	3.9117	2.9191	35.072	3.644	1.5796	2.5715
Ava.	**1.15467**	2.12200	**0.6513**	14.578	3.1150	3.5892	2.6955	28.87	3.798	**1.4507**	**1.6065**

Each algorithm was rigorously tested and compared to shed light on its strengths and weaknesses. The results provide valuable insights for image processing applications and highlight the need for further optimization in certain areas. The WCD algorithm delivered a bad performance, with more need to improve colors and amplify the brightness. and was ranked 3rd fastest method. In addition, the UDCP algorithm provided adequate colors with dark and unclear details. and was slow by scoring the 9th rank. Moreover, the BLA algorithm delivered a poor performance and an increase in contrast without any noticeable change in results, and it was ranked last in terms of speed because it involves many operations. Furthermore, the TSA algorithm provided with dark appearance, Still, it ranked the 6th fastest method. Moreover, the DHW Algorithm delivered an unpleasant performance, the image appears dark, details and colors are blurred, increasing color distortion, and ranked 8th in terms of speed. Furthermore, the GIF algorithm delivered a somewhat low performance, as it worked well with images that have more of a blue color composition and, an increase in white balance, and ranked the 7th fastest among the comparison methods. Furthermore, the HF algorithm delivered moderate performances by improving the contrast and saturation and ranked 10th in terms of speed. Furthermore, the HA algorithm delivered low performances with more need for color optimization and brightness adjustment. while being the fastest method. Moreover, the MWMGF algorithm delivered an above-moderate performance, with a balanced

contrast, a greater need for color optimization and brightness adjustment, blur appearance, and some noise amplification, and ranked 5th fastest method. Furthermore, the CBF algorithm delivered low performances, with more needed for color optimization and brightness adjustment, and ranked 2nd in terms of speed.

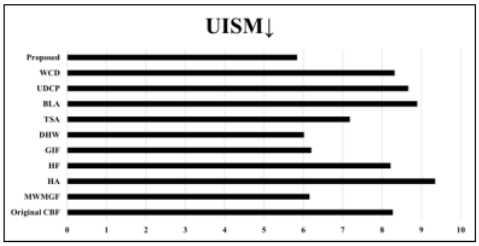

Figure 13. The average readings of the UISM.

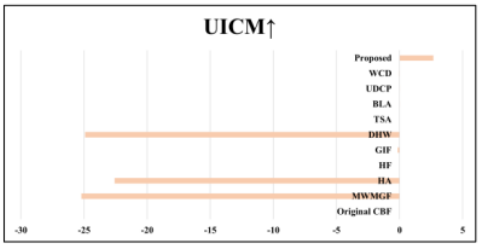

Figure 14. The average readings of the UICM.

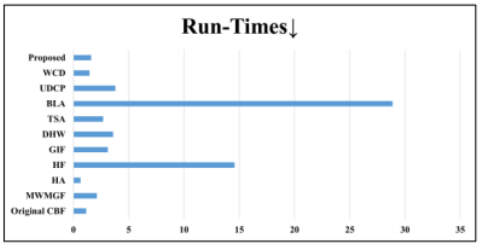

Figure 15. The average runtimes of the comparison methods.

In summary, these findings provide valuable guidance for selecting image enhancement algorithms based on specific requirements. Researchers and practitioners can use this information to make informed decisions regarding algorithm choices for different image-processing applications. Further research and development are encouraged to address the identified limitations and improve the overall performance of these algorithms.

V. Conclusion

This study introduced a multi-process methodology for underwater image enhancement. The methodology utilizes different processes and then blends the outcomes to produce the output image. The introduced methodology has been tested with many different images captured in unfavorable underwater conditions. Moreover, it has been compared with ten different methodologies, and a thorough analysis has been provided. The comparison outcomes have been assessed with two methods specifically designed for underwater images. From these actions, the proposed methodology showed promising results as it was able to process various images captured by different cameras, depths, and lighting conditions and can provide better colors, quality, and visibility for the details seen in the processed images. Moreover, it performed well when compared to other methods by outperforming ten existing methods. This is a solid achievement as developing a legacy method to become better was fruitful as proven by the obtained results.

VI. References

[1] Lavy, A., Eyal, G., Neal, B., Keren, R., Loya, Y., & Ilan, M. (2015). A quick, easy and non-intrusive method for underwater volume and surface area evaluation of benthic organisms by 3D computer modelling. Methods in Ecology and Evolution, 6(5), 521-531.

[2] Pacheco-Ruiz, R., Adams, J., & Pedrotti, F. (2018). 4D modelling of low visibility Underwater Archaeological excavations using multi-source photogrammetry in the Bulgarian Black Sea. Journal of Archaeological Science, 100, 120-129.

[3] Wu, X., Xiao, L., Sun, Y., Zhang, J., Ma, T., & He, L. (2022). A survey of human-in-the-loop for machine learning. Future Generation Computer Systems, 135, 364-381.

[4] Dewangan, S. K. (2017, May). Visual quality restoration & enhancement of underwater images using HSV filter analysis. In 2017 International Conference on Trends in Electronics and Informatics (ICEI) (pp. 766-772). IEEE

[5] Hambarde, P., Murala, S., & Dhall, A. (2021). UW-GAN: Single-image depth estimation and image enhancement for underwater images. IEEE Transactions on Instrumentation and Measurement, 70, 1-12.

[6] Rajasekar, M., Celine Kavida, A., & Anto Bennet, M. (2020). A pattern analysis based underwater video segmentation system for target object detection. Multidimensional Systems and Signal Processing, 31, 1579-1602.

[7] Liu, Y., Xu, H., Shang, D., Li, C., & Quan, X. (2019). An underwater image enhancement method for different illumination conditions based on color tone correction and fusion-based descattering. Sensors, 19(24), 5567.

[8] Butler, J., Stanley, J. A., & Butler IV, M. J. (2016). Underwater soundscapes in near-shore tropical habitats and the effects of environmental degradation and habitat restoration. Journal of Experimental Marine Biology and Ecology, 479, 89-96.

[9] Liu, X., Guillén, I., La Manna, M., Nam, J. H., Reza, S. A., Huu Le, T., ... & Velten, A. (2019). Non-line-of-sight imaging using phasor-field virtual wave optics. Nature, 572(7771), 620-623.

[10] Schöntag, P., Nakath, D., Röhrl, S., & Köser, K. (2022, May). Towards Cross Domain Transfer Learning for Underwater Correspondence Search. In International Conference on Image Analysis and Processing (pp. 461-472). Cham: Springer International Publishing.

[11] Chiang, J. Y., & Chen, Y. C. (2011). Underwater image enhancement by wavelength compensation and dehazing. IEEE transactions on image processing, 21(4), 1756-1769.

[12] Drews, P., Nascimento, E., Moraes, F., Botelho, S., & Campos, M. (2013). Transmission estimation in underwater single images. In Proceedings of the IEEE international conference on computer vision workshops (pp. 825-830).

[13] Peng, Y. T., & Cosman, P. C. (2017). Underwater image restoration based on image blurriness and light absorption. IEEE Transactions on Image Processing, 26(4), 1579-1594.

[14] Fu, X., Fan, Z., Ling, M., Huang, Y., & Ding, X. (2017, November). Two-step approach for single underwater image enhancement. In 2017 International Symposium on Intelligent Signal Processing and Communication Systems (ISPACS) (pp. 789-794). IEEE.

[15] Pan, P. W., Yuan, F., & Cheng, E. (2018). Underwater image de-scattering and enhancing using dehazenet and HWD. Journal of Marine Science and Technology, 26(4), 6.

[16] Bavirisetti, D. P., Xiao, G., Zhao, J., Dhuli, R., & Liu, G. (2019). Multi-scale guided image and video fusion: A fast and efficient approach. Circuits, Systems, and Signal Processing, 38, 5576-5605.

[17] Li, X., Hou, G., Tan, L., & Liu, W. (2020). A hybrid framework for underwater image enhancement. IEEE Access, 8, 197448-197462.

[18] Fayaz, S., Parah, S. A., & Qureshi, G. J. (2023). Efficient underwater image restoration utilizing modified dark channel prior. Multimedia Tools and Applications, 82(10), 14731-14753.

[19] Wang, S., Chen, Z., & Wang, H. (2022). Multi-weight and multi-granularity fusion of underwater image enhancement. Earth Science Informatics, 15(3), 1647-1657.

[20] Ancuti, C. O., Ancuti, C., De Vleeschouwer, C., & Bekaert, P. (2017). Color balance and fusion for underwater image enhancement. IEEE Transactions on image processing, 27(1), 379-393.

[21] Goldstein, E. B. (Ed.). (2009). Encyclopedia of perception. Sage.

[22] Huang, Z., Fang, H., Li, Q., Li, Z., Zhang, T., Sang, N., & Li, Y. (2018). Optical remote sensing image enhancement with weak structure preservation via spatially adaptive gamma correction. Infrared Physics & Technology, 94, 38-47.

[23] Yang, X., Yin, C., Zhang, Z., Li, Y., Liang, W., Wang, D., ... & Fan, H. (2020). Robust chromatic adaptation based color correction technology for underwater images. Applied Sciences, 10(18), 6392.

[24] Ma, S., Hanselaer, P., Teunissen, K., & Smet, K. A. (2020). Effect of adapting field size on chromatic adaptation. Optics Express, 28(12), 17266-17285.

[25] Rahman, S., Rahman, M. M., Abdullah-Al-Wadud, M., Al-Quaderi, G. D., & Shoyaib, M. (2016). An adaptive gamma correction for image enhancement. EURASIP Journal on Image and Video Processing, 2016(1), 1-13.

[26] Rao, N., Venkatasekhar, D., Venkatramana, P., & Usha Rani, C. (2019). Optical Features Based Fusion Principle for Under Water Image Enhancement. Journal of Computational and Theoretical Nanoscience, 16(4), 1227-1233.

[27] Achanta, R., Hemami, S., Estrada, F., & Susstrunk, S. (2009, June). Frequency-tuned salient region detection. In 2009 IEEE conference on computer vision and pattern recognition (pp. 1597-1604). IEEE.

[28] Parihar, A. S., Singh, K., Rohilla, H., & Asnani, G. (2021). Fusion-based simultaneous estimation of reflectance and illumination for low-light image enhancement. IET Image Processing, 15(7), 1410-1423.

[29] Al-Ameen, Z. (2020). Satellite Image Enhancement Using an Ameliorated Balance Contrast Enhancement Technique. Traitement du Signal, 37(2).

[30] Al-Ameen, Z., Al-Healy, M. A., & Hazim, R. A. (2020). Anisotropic Diffusion-Based Unsharp Masking for Sharpness Improvement in Digital Images. Journal of Soft Computing & Decision Support Systems, 7(1).

[31] Zhang, W., Dong, L., Pan, X., Zhou, J., Qin, L., & Xu, W. (2019). Single image defogging based on multi-channel convolutional MSRCR. IEEE Access, 7, 72492-72504.

[32] Huang, Z., Fang, H., Li, Q., Li, Z., Zhang, T., Sang, N., & Li, Y. (2018). Optical remote sensing image enhancement with weak structure preservation via spatially adaptive gamma correction. Infrared Physics & Technology, 94, 38-47.

[33] Li, C., Guo, C., Ren, W., Cong, R., Hou, J., Kwong, S., & Tao, D. (2019). An underwater image enhancement benchmark dataset and beyond. IEEE Transactions on Image Processing, 29, 4376-4389.

Low Intricacy Multistage Algorithm for Underwater Image Enhancement

ORIGINALITY REPORT

13%	10%	11%	2%
SIMILARITY INDEX	INTERNET SOURCES	PUBLICATIONS	STUDENT PAPERS

PRIMARY SOURCES

1	iieta.org Internet Source	2%
2	ph.pollub.pl Internet Source	2%
3	link.springer.com Internet Source	1%
4	mafiadoc.com Internet Source	1%
5	www.mdpi.com Internet Source	1%
6	journal.uad.ac.id Internet Source	1%
7	Submitted to Universitas Khairun Student Paper	<1%
8	www.researchgate.net Internet Source	<1%
9	P. R. Dhanya, Syamily Anilkumar, Arun A. Balakrishnan, M. H. Supriya. "L-CLAHE	<1%

	Intensification Filter (L-CIF) Algorithm for Underwater Image Enhancement and Colour Restoration", 2019 International Symposium on Ocean Technology (SYMPOL), 2019 Publication	
10	Aswathy Sukumaran, Ajith Abraham. "Automated Detection and Classification of Meningioma Tumor from MR Images Using Sea Lion Optimization and Deep Learning Models", Axioms, 2021 Publication	<1 %
11	Zohair Al-Ameen. "Satellite Image Enhancement Using an Ameliorated Balance Contrast Enhancement Technique", Traitement du Signal, 2020 Publication	<1 %
12	repository.uin-suska.ac.id Internet Source	<1 %
13	dokumen.pub Internet Source	<1 %
14	www.frontiersin.org Internet Source	<1 %
15	www.iieta.org Internet Source	<1 %
16	www.semanticscholar.org Internet Source	<1 %

17	"Computational Vision and Bio-Inspired Computing", Springer Science and Business Media LLC, 2022 Publication	<1 %
18	Weidong Zhang, Lili Dong, Wenhai Xu. "Retinex-inspired color correction and detail preserved fusion for underwater image enhancement", Computers and Electronics in Agriculture, 2022 Publication	<1 %
19	Xinjie Li, Guojia Hou, Lu Tan, Wanquan Liu. "A Hybrid Framework for Underwater Image Enhancement by Dehazing", IEEE Access, 2020 Publication	<1 %
20	"Computational Intelligence in Pattern Recognition", Springer Science and Business Media LLC, 2020 Publication	<1 %
21	Zohair Al-Ameen. "Nighttime image enhancement using a new illumination boost algorithm", IET Image Processing, 2019 Publication	<1 %
22	"Advances in Multimedia Information Processing – PCM 2018", Springer Science and Business Media LLC, 2018 Publication	<1 %

23	Submitted to Jacobs University, Bremen Student Paper	<1 %
24	jivp-eurasipjournals.springeropen.com Internet Source	<1 %
25	www.ijraset.com Internet Source	<1 %
26	I. Cosovic, S. Brandes, M. Schnell. "Subcarrier weighting: a method for sidelobe suppression in OFDM systems", IEEE Communications Letters, 2006 Publication	<1 %
27	Peixian Zhuang, Chongyi Li, Jiamin Wu. "Bayesian retinex underwater image enhancement", Engineering Applications of Artificial Intelligence, 2021 Publication	<1 %
28	dspace.library.uvic.ca Internet Source	<1 %
29	"Artificial Intelligence and Security", Springer Science and Business Media LLC, 2020 Publication	<1 %
30	"Intelligent Systems Design and Applications", Springer Science and Business Media LLC, 2020 Publication	<1 %

31	Deepak Kumar Rout, Badri Narayan Subudhi, T. Veerakumar, Santanu Chaudhury, John Soraghan. "Multiresolution visual enhancement of hazy underwater scene", Multimedia Tools and Applications, 2022 Publication	<1 %
32	Zohair Al-Ameen. "Contrast Enhancement of Digital Images Using an Improved Type-II Fuzzy Set-Based Algorithm", Traitement du Signal, 2021 Publication	<1 %
33	Shuqi Wang, Zhixiang Chen, Hui Wang. "Multi-weight and multi-granularity fusion of underwater image enhancement", Earth Science Informatics, 2022 Publication	<1 %

Exclude quotes	Off	Exclude matches	Off
Exclude bibliography	On		